

MOLECULAR CONFORMATIONS OF CEREBROSIDES IN BILAYERS DETERMINED BY RAMAN SPECTROSCOPY

MARGARET R. BUNOW AND IRA W. LEVIN, *Laboratory of Chemical Physics,
National Institute of Arthritis, Metabolism and Digestive Diseases, National
Institutes of Health, Bethesda, Maryland 20205 U.S.A.*

ABSTRACT Vibrational Raman spectra of the solid and gel phases of bovine brain cerebroside and the component fractions, kerafin and phrenosin, provide conformational information for these glycosphingolipids in bilayer systems. The carbon-carbon stretching mode profiles ($1,150\text{--}1,000\text{ cm}^{-1}$) indicate that at 22°C the alkyl chains assume an almost all-*trans* arrangement. These spectral data, combined with those from the C-H stretching region ($3,050\text{--}2,800\text{ cm}^{-1}$), show that phrenosin forms the most highly ordered polycrystalline solid and kerafin the most ordered gel phase. The conformation of the unsaturated, 24-carbon acyl chains is monitored independently by a skeletal stretching mode at $1,112\text{ cm}^{-1}$. The alkyl chains in the kerafin and phrenosin gels are sufficiently extended to allow interdigitation of the 24-carbon acyl chains across the midplane of the bilayer. The amide I vibrational mode occurs at a lower frequency in solid phrenosin than kerafin, a shift consistent with stronger hydrogen bonding. This band is broadened and shifted to higher frequencies, however, in the phrenosin gel phase. In both the solid and gel phases natural cerebroside exhibits a composite amide I mode. The disruptive effects on cerebroside chain packing and headgroup orientation arising from mixing with dimyristoyl phosphatidylcholine are examined. Vibrational data for cerebroside are also compared to those for ceramide, sphingosine, and distearoyl phosphatidylcholine structures. Spectral interpretations are discussed in terms of calorimetric and x-ray structural data.

INTRODUCTION

The sphingolipids compose a major class of plasma membrane lipids. Among these, bovine brain cerebroside, especially those from white matter, contain predominantly long-chain ($\text{C}_{18}\text{--}\text{C}_{26}$) fatty acids linked to the C_{18} sphingosine moiety (see Fig. 1). The long-chain character of the fatty acyl groups, combined with the extensive hydrogen bonding capacity of the galactose headgroup and the adjacent polar region of the molecule, is presumed to confer great stability on bilayers of this lipid (1) and may account for the utilization of galactolipids as the major lipid by weight in the myelin membrane. Myelin contains lipids in the molar proportions of 1:1.5:2 for cerebroside, phospholipid, and cholesterol, respectively (2).

A complete structure determination for a crystalline phrenosin (1), as well as data on bilayers with and without water (3), is available from x-ray data. In the present paper, we describe various conformational features of cerebroside bilayers as determined by vibrational Raman spectroscopy, a technique which allows a direct comparison between crystalline

Dr. Bunow's present address is the Laboratory of Chemical Carcinogenesis, NCI, NIH, Bethesda, Md. 20205.

(anhydrous) and hydrated bilayers without significant interference from the spectrum of water. These structural features involve both chain packing and headgroup conformational arrangements.

MATERIALS AND METHODS

Bovine brain cerebroside, kerosin (β -D-galactosyl-*N*-(*n*-acyl)-D-sphingosine), phrenosin (β -D-galactosyl-*N*-(2-D-hydroxyacyl)-D-sphingosine), sphingosine, and D-galactose, (98% pure) were obtained from P-L Biochemicals, Milwaukee, Wisc.; ceramide and other samples of cerebroside (>98% pure) from Supelco, Inc., Bellefonte, Pa.; L- α -dimyristoyl phosphatidylcholine (DMPC) from Calbiochem, Inc., San Diego, Calif.; DL- α -distearoyl phosphatidylcholine (DSPC) from Sigma Chemical Co., St. Louis, Mo., and *N*-lignoceryl-DL-dihydrogalactocerebroside from Miles Labs, Inc., Elkhart, Ind. All samples were used without further purification.

Solid state samples were dried under vacuum, sealed in melting point capillaries, and annealed by thermal cycling from -180°C to room temperature. Gel state samples of the cerebroside were mixed with excess water (50% by weight) at temperatures above the gel to liquid crystalline phase transition temperature (65° – 72°C [4]), sealed in melting point capillaries, spun in a tube (hematocrit) centrifuge, and then annealed. The kerosin gel was also equilibrated overnight at -20°C to attain a stable state (4). Kerosin-DMPC mixtures were prepared by dissolving in chloroform-methanol solutions, followed by thorough drying *in vacuo* and hydration with mechanical mixing at temperatures above the gel to liquid crystalline phase transition. Mole fractions, X , were computed from the weights of the components, assuming molecular weights of 814 for kerosin and 696 for DMPC. Vibrational Raman spectra of samples were obtained using excitation of ~ 250 mW at 514.5 nm of a Coherent Model CR-3 argon ion laser (Coherent Radiation, Palo Alto, Calif.) and a Spex Ramalog 6 spectrometer (Spex Industries, Metuchen, N.J.) equipped with NIC-1180 data system (Madison, Wisc.) for spectral accumulations. Preliminary spectra were obtained using a Cary Model 81 double monochromator (Varian Instrument Co., Palo Alto, Calif.) equipped with modified sample and entrance optics and a modified detection system. Spectral resolution was of the order of $2\text{--}3\text{ cm}^{-1}$. Spectral frequencies, calibrated with atomic argon lines, are reported to $\pm 2\text{ cm}^{-1}$. Sample temperatures were controlled using either a gaseous nitrogen stream passed through a copper coil in contact with an appropriate temperature bath or a thermostatically controlled sample holder.

Unless otherwise noted, spectral ratios were computed from band height measurements. Band area ratios, where used, were computed from the spectral band halfwidths and band heights.

To identify the solid phases, the thermal behavior of 2-mg samples of solid phases, annealed at -180°C and sealed into aluminum pans, was examined by differential scanning calorimetry. Heating and cooling scans at $5^{\circ}\text{C min}^{-1}$ were recorded on a Perkin-Elmer DSC-2 instrument (Perkin-Elmer, Norwalk, Conn.). A set of both endothermic and exothermic phase transitions was recorded for each sample as a function of increasing temperature. The reversibility of transitions was examined in cooling scans.

RESULTS

Raman spectra of both the solid state and gel phases of bovine brain cerebroside, kerosin, and phrenosin were recorded. To verify spectral assignments and conformational behavior, solid phase ceramide, sphingosine, D-galactose, and kerosin equilibrated with D_2O were also examined. The cerebroside phases were further characterized by their calorimetrically detected phase transitions. Molecular structures of the sphingolipids are given in Fig. 1.

Bovine brain cerebroside contains roughly equal amounts of the kerosin and phrenosin fractions, differentiated by 2-hydroxyl substitution of the fatty acid chains of phrenosin. The major fatty acids in bovine brain kerosin are C24:1, 40%; C24:0, 17%; and C18:0, 6%;

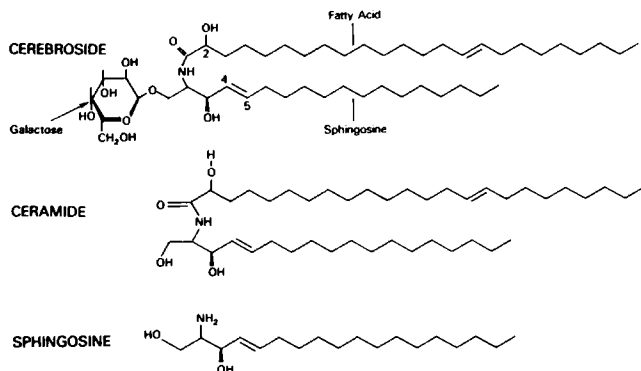


FIGURE 1 Molecular structures of cerebroside and the reference compounds ceramide and sphingosine. The cerebroside is shown as a phrenosin, with a 2-OH group on the acyl chain. The fatty acid composition of bovine brain cerebroside is given in Results; the 15,16-*cis* unsaturation of the acyl chain shown in the figure is much more prevalent in the kersin (β -D-galactosyl-*N*-(*n*-acyl)-D-sphingosine) fraction than the phrenosin (β -D-galactosyl-*N*-(2-D-hydroxyacyl)-D-sphingosine) fraction of cerebroside.

compared to phrenosin containing (hydroxy-) C24:1, 15%; C24:0, 30%; and C18:0, 16% (5). The precise numbers vary with the preparation (6, 7), but the pattern of a relatively greater unsaturation of C24 fatty acids in kersin as compared to phrenosin is always retained (2). The predominant *cis* unsaturated fatty acid species is nervonic acid (C24:1) with a 15,16-*cis* double bond (8). The contribution of all other, minor components occurring at the 5% level (5–7) is discussed below.

In the Raman spectra of lipids, the alkyl chains contribute vibrational modes involving methylene CH_2 stretching ($3,050\text{--}2,800\text{ cm}^{-1}$), CH_2 deformation ($1,480\text{--}1,400\text{ cm}^{-1}$), CH_2 twisting ($1,300\text{ cm}^{-1}$) and $\text{C}\text{--}\text{C}$ skeletal stretching ($1,150\text{--}1,000\text{ cm}^{-1}$) motions. For these modes, peak height intensity ratios, band widths, and vibrational frequencies have been established as parameters reflecting chain conformation and chain interaction (9–12). The $1,700\text{--}1,600\text{ cm}^{-1}$ spectral region contains $\text{C}=\text{C}$ stretching modes, which include those of the 4,5-*trans* double bond near the polar headgroup in the sphingosine moiety of the sphingolipid molecules, and the amide $\text{C}=\text{O}$ stretching mode, which monitors the conformation at the linkage between the sphingosine and fatty acid chains in the polar end of the molecule.

The 3,100- to 2,800- cm^{-1} Region

The $\text{C}\text{--}\text{H}$ stretching region ($3,100\text{--}2,800\text{ cm}^{-1}$) in the Raman spectra of lipids is dominated primarily by contributions from the methylene symmetric and antisymmetric CH_2 stretching mode fundamentals which are perturbed by a Fermi resonance interaction between the symmetric $\text{C}\text{--}\text{H}$ stretching mode and a continuum of overtones involving the methylene CH_2 deformation modes (13). As a consequence, the 3,100- to 2,800- cm^{-1} profile senses both intrachain conformations and lateral, interchain interactions (9, 10). The 3,100- to 2,800- cm^{-1} region for all the cerebroside is not reproduced here, but the survey spectra in Fig. 2 display the difference in the 2,850- cm^{-1} bandwidths for the solid phase cerebroside compared to that for solid phase ceramide.

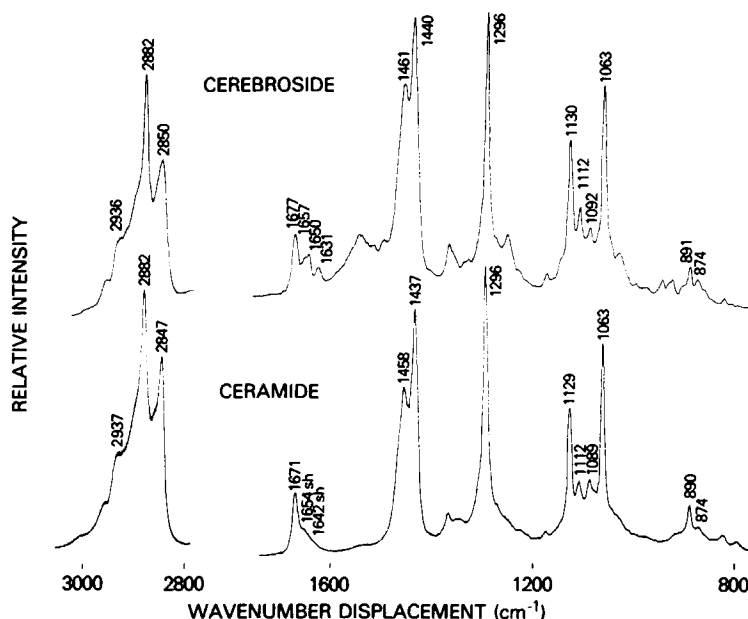


FIGURE 2 Survey Raman spectra for (top) annealed crystalline bovine brain cerebroside and (bottom) ceramide in the 3,050- to 2,800- cm^{-1} and 1,700- to 800- cm^{-1} regions. Noteworthy is the essential similarity of the two spectra in terms of the profiles in the 3,050- to 2,800- cm^{-1} and 1,150- to 1,000- cm^{-1} regions, reflecting hydrocarbon chain dominance of the spectra. The width of the 2,850- cm^{-1} peak is greater in cerebroside than ceramide (see text). The amide I band shows more structure in cerebroside than ceramide. The intensity scale of the 3,050- to 2,800- cm^{-1} region for both compounds is compressed about three times relative to the rest of the spectra. sh, shoulder.

The width of the band at 2,850 cm^{-1} (the methylene CH_2 symmetric stretching modes) is affected by a Fermi resonance with the overtones of the methylene CH_2 deformation modes (13). The width at three quarters height, $\Delta\nu_{3/4}(2,850)$, of this mode is plotted for the different cerebroside in Figs. 3 and 4. Although it is customary to consider the halfwidth of spectral bands, the actual width defined at three quarters height, $\Delta\nu_{3/4}(2,850)$, is readily obtained in the present case without an ambiguous deconvolution. The broadest bands are seen for the solid phase cerebroside and for the gel phase of kersin; in contrast, the 2,850- cm^{-1} peak is remarkably narrower for the gel phase of phrenosin compared to the polycrystalline solid. For reference, the 2,850- cm^{-1} band width for the gel phase of DSPC at 25°C is given in Fig. 4. In saturated-chain diacyl phosphatidylcholine gels, the 2,850- cm^{-1} band broadens as the temperature drops, reflecting, in part, the resonance effects of shorter interchain distances in the contracting gel. The solid state cerebroside and the kersin gel at 22°C exhibit 2,850- cm^{-1} bands markedly wider than that of the DSPC gel at -180°C, (>20 compared to 15.8 cm^{-1}) which is suggestive of chain lattices more contracted than that of DSPC. Solid state ceramide and sphingosine exhibit narrower 2,850- cm^{-1} peaks. At low temperatures the lecithin gels also exhibit a 1,420- cm^{-1} shoulder on the methylene deformation modes, characteristic of an orthorhombic hydrocarbon chain lattice. This shoulder is not, however, seen in spectra of the cerebroside at room temperature.

The ratios of peak height intensities, at 2,880 and 2,935 cm^{-1} , $h_{2,880}/h_{2,935}$, for all

and such plots for the present systems produce very complex ratios which are not simple functions of relative chain order (plots not shown).

The peak height intensity ratios $h_{2,880}/h_{2,935}$ identify phrenosin as the system which forms the most highly ordered crystal, while keraasin develops the most highly ordered gel state. The peak height ratios for the keraasin and phrenosin gels at 22°C are comparable to those recorded for DSPC gels at 25° and 34°C, respectively. (The gel to liquid crystalline phase transition temperature for this lecithin is 54°C.)

The 1,700- to 1,600-cm⁻¹ Region

Both the C=C stretching modes and the amide I band occur within the 1,700- to 1,600-cm⁻¹ region in the spectra for the cerebroside (Fig. 5). The 1,673-cm⁻¹ Raman band represents the

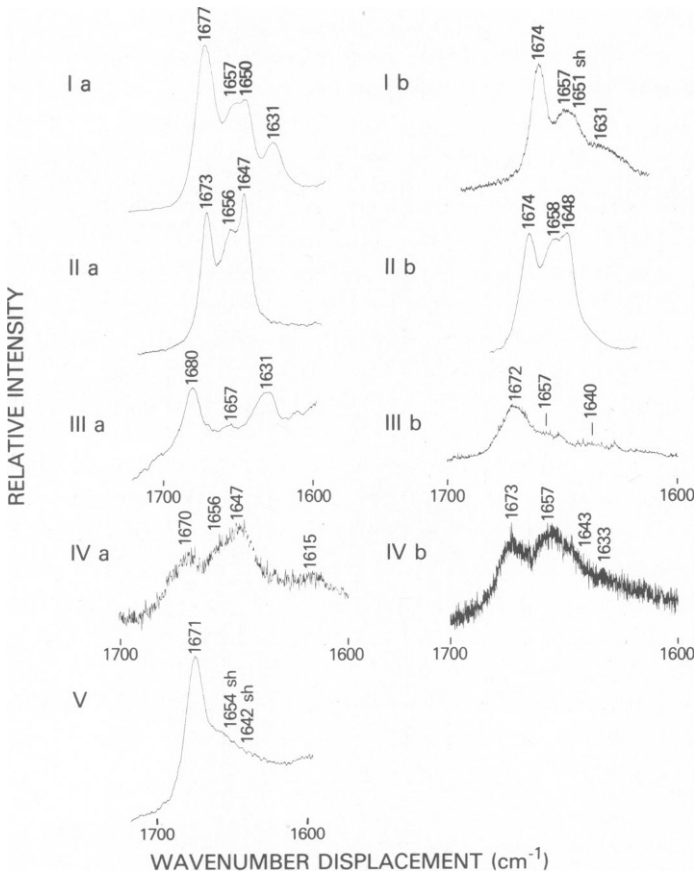


FIGURE 5 The 1,700- to 1,600-cm⁻¹ region of the Raman spectra of (I) cerebroside in (a) solid and (b) gel phases; (II) keraasin in (a) solid and (b) gel phases; (III) phrenosin in (a) solid and (b) gel phases, all at 22°C; (IV) keraasin-DMPC mixture at (a) $X_k = 0.7$, 25°C, gel phase and (b) $X_k = 0.29$, 29°C, gel plus liquid crystalline phases in equilibrium; and (V) solid phase ceramide, where the wavenumbers on shoulders were obtained by deconvolution of the region (not shown). IIIb, IVa, and IVb are signal averaged spectra; the wavenumber scales on these spectra differ from the others. Spectral intensities are not normalized among the different spectra. sh, shoulder.

C=C stretching vibration associated with the 4,5-*trans* double bond of the sphingosine moiety. It was found to have a fairly constant intensity ratio (based on band areas) relative to that of the methylene deformation modes at $1,450\text{ cm}^{-1}$. The ratio varies from 0.08 to 0.12 with the species of glycolipid. The intensity ratio in the single-chain sphingosine was 0.27, in reasonable accord with the ratio of methylene carbons in sphingosine relative to the cerebroside. The frequency of the C=C mode was higher in solid phase phrenosin than kerasin, $1,680$ vs. $1,673\text{ cm}^{-1}$, and at an intermediate value, $1,677\text{ cm}^{-1}$, in natural cerebroside (Fig. 5). The bandwidth in the latter ($\Delta\nu_{1/2} = 15.6\text{ cm}^{-1}$) was greater than that in the solid phases of phrenosin and kerasin ($\Delta\nu_{1/2} = 11.7\text{ cm}^{-1}$ in kerasin and $\Delta\nu_{1/2} = 13.8\text{ cm}^{-1}$ in phrenosin), which is consistent with the band in the cerebroside being a composite of those in the cerebroside fractions. The different frequencies for the C=C stretching mode indicate inequivalent conformational and environmental effects at the 4,5 carbon level near the polar surface of the ordered arrays of cerebroside molecules in the solid phase. In contrast, for the gel phase of the cerebroside, the C=C stretching mode frequencies are the same, $1,673$ – $1,674\text{ cm}^{-1}$ (Fig. 5).

The $1,657\text{-cm}^{-1}$ band in the cerebroside spectra was assigned to the C=C stretching mode associated with *cis*-unsaturation of the acyl chains as a consequence of its frequency, absence in sphingosine and insensitivity to D_2O exposure. Since the intensity of this mode was three times greater in kerasin than phrenosin, it was considered to give a good estimate of these fractions' relative *cis*-unsaturation (vide supra for acyl chain composition).

The amide I band, reflecting C=O in-plane stretching plus in-plane N—H bending, is associated with the amide linkage between the sphingosine and the fatty acid chains. It appears at $1,647\text{ cm}^{-1}$ in solid phase kerasin ($1,638\text{ cm}^{-1}$ after D_2O exposure) and at $1,631\text{ cm}^{-1}$ in solid phase phrenosin. A composite amide I band is observed in cerebroside, at $1,645$ and $1,630\text{ cm}^{-1}$, indicating the existence of the two different bond conformations characteristic of the kerasin and phrenosin headgroups, respectively, in the natural cerebroside mixture. Similar profiles are seen for the solid and gel phases of kerasin upon hydration. In the phrenosin gel, however, the $1,631\text{-cm}^{-1}$ band is broadened and shifted upward to $1,640 \pm 5\text{ cm}^{-1}$, which indicates a more extensive breakdown of the inter- and intramolecular hydrogen-bonding scheme (Fig. 5). This shift upon hydration was not previously detected, but is evident in signal averaged spectra. For comparison, in solid samples of ceramide, a very broad amide I band occurred at $1,642\text{ cm}^{-1}$, which suggests an increased conformational freedom in the absence of the galactose headgroup (Figs. 2 and 5). A very weak background due to water and centered at $1,620\text{ cm}^{-1}$ may underlie this region of the spectra of gel phases.

The 1,500- to 1,400- cm^{-1} Region

The methylene CH_2 deformation modes centered at $\sim 1,450\text{ cm}^{-1}$ are composed predominantly of alkyl chain contributions. Plots of the inverse of the halfwidth of these modes, $\Delta\nu_{1/2}(1,450)$, an order parameter, again show that phrenosin forms the most highly ordered solid and kerasin the most ordered gel (Figs. 3 and 4). The extraordinarily high value of this parameter for gel phase kerasin indicates a very ordered, compact alkyl chain lattice with a restricted distribution of methylene CH_2 deformation modes.

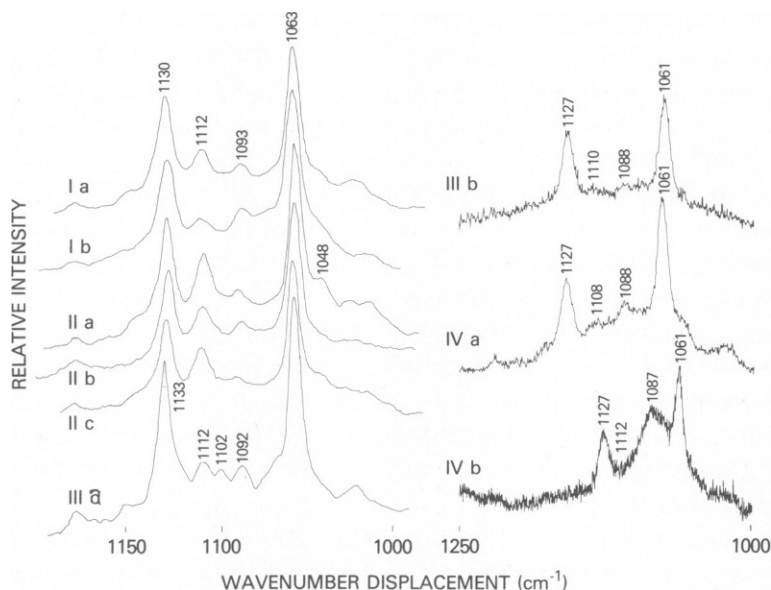


FIGURE 6 The C—C skeletal stretching region (1,150–1,000 cm^{-1}) of the Raman spectra of (I) bovine brain cerebroside in (a) solid and (b) gel states; (II) kerosin in (a) solid state and (b) solid state after equilibration with D_2O and (c) gel state; (III) phrenosin in (a) solid and (b) gel states; and (IV) kerosin-DMPC mixtures at (a) $X_k = 0.7$, 25°C and (b) $X_k = 0.29$ 29°C . IIIb, IVa, and IVb are signal averaged spectra. Note that the wavenumber scales on these spectra differ. Temperature was 22°C except as noted. Spectral conditions are as in Fig. 5.

The 1,150- to 1,000- cm^{-1} Region

Fig. 6 shows the Raman spectral profiles in the 1,150- to 1,000- cm^{-1} region for the cerebroside. Figs. 3 and 4 display the peak height ratios $(h_{1,132} + h_{1,112})/h_{1,088}$ and $h_{1,062}/h_{1,088}$. These ratios are used to reflect the content of all-*trans* chain conformers relative to the *gauche* conformer content, as explained below. Comparisons of the spectrum of cerebroside to that of ceramide (Fig. 2), and of kerosin to kerosin exposed to D_2O (Fig. 6), indicate that the galactose moiety and other groups containing exchangeable hydrogens do not alter the profile in the region 1,140–1,050 cm^{-1} , but do contribute a weak background as well as weak features at $\sim 1,143$, 1,048, and 1,034 cm^{-1} . To minimize these contributions, the baseline for determining peak heights in the C—C stretching region was taken as the chord between 1,170 and 1,040 cm^{-1} .

A band associated with C—C skeletal stretching vibrations of *gauche* conformers occurs at the reference frequency of 1,088 cm^{-1} (11, 15); its position in cerebroside has been verified by perturbation of the chain packing of kerosin and phrenosin gels by addition of CHCl_3 or the I^- ion (spectra not shown).

The 1,062- cm^{-1} mode, a nearly pure C—C stretching mode, is insensitive to chain length and unsaturation (11, 15); its bandshape provides a good parameter of average all-*trans* chain conformer content. The 1,132- cm^{-1} mode has been shown for fatty acids to reflect all-*trans* chain conformers for both fatty acid chain segments longer than 14 carbons which terminate in a methyl group, and chain segments longer than 20 carbons bounded at opposite ends by

carboxyl and double bond groups (15). The frequencies for shorter chain segments of both types decrease rapidly, but at different rates, with decreasing chain segment length (15). We assume that the amide bond constraint at the polar end of the acyl chain in cerebrosides is equivalent to the carboxyl group constraint of fatty acids, and adopt the assignments from the latter systems.

The ratio of the band area at $1,132\text{ cm}^{-1}$ to that of relatively invariant $1,060\text{-cm}^{-1}$ mode is 25% higher in solid phase phrenosin than kersin, largely because the proportion of long chains satisfying the length relations just described for the $1,130\text{-cm}^{-1}$ mode is greater in phrenosin than kersin. Besides the major (hydroxy-) C18:0 and C24:0 chains, phrenosin also contains (hydroxy-) C22:0, C23:0, and C25:0 chains at the 5% level (5–7). These chains all contribute to the $1,132\text{-cm}^{-1}$ mode. In kersin, the acyl chains are more frequently interrupted by a *cis*-double bond located at or beyond carbon 15 (*vide supra*).

The band at $1,112\text{ cm}^{-1}$ is tentatively assigned to the all-*trans* conformers of the 15-carbon chain segment between the amide group and the double bond, as well as the all-*trans* segments lying between the double bond and the methyl end of the nervonic acid (C24:1) chain. Besides C24:1, kersin and phrenosin also contain ~5% C25:1 and C26:1 chains (5–7). By normal mechanisms of chain lengthening (16), the predominant methyl-terminated chain segments are seven and nine carbons long (eight for the odd length chain) below the double bond, while the chain segments between the amide and double bond are 16 to 19 carbons long. This distribution of chain segment lengths around the major nervonic acid component has the effect of broadening the $1,112\text{-cm}^{-1}$ peak (Fig. 6). The assignment of the $1,112\text{-cm}^{-1}$ mode is based on studies of solid state fatty acids (Fig. 7 of reference 15). (Recently [4], one of us pointed out the association of the $1,112\text{-cm}^{-1}$ mode with the conformation of the seven- to

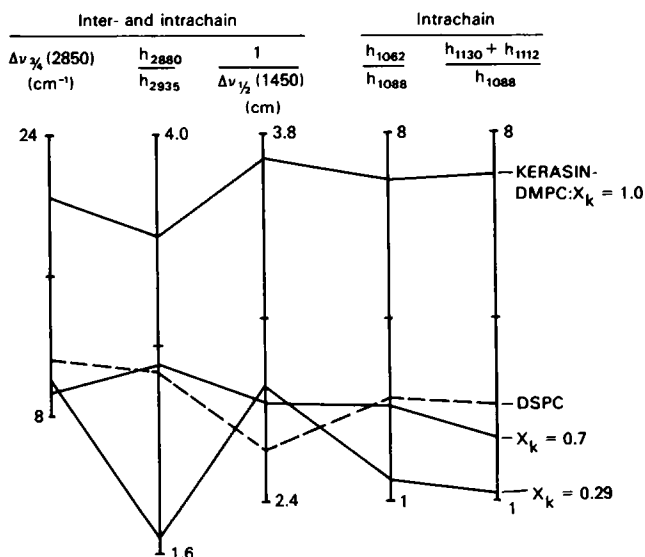


FIGURE 7 Order parameters derived from Raman spectral profiles for gel phase kersin at 22°C , $X_k = 1.0$; gel phase of kersin-DMPC at 25°C , $X_k = 0.7$; and gel plus liquid crystalline phases of kersin-DMPC, 29°C , $X_k = 0.29$ (solid lines); and gel phase of DSPC, 39°C (dashed line). Scaling is not identical to that in Figs. 3 and 4.

nine-carbon terminus, but not the probable complexity of this spectral feature.) The band at $1,112\text{ cm}^{-1}$ is twice as intense, relative to the $1,062\text{-cm}^{-1}$ mode, in kersin than phrenosin. This intensity relation is in rough proportion to the intensity of the $\text{C}=\text{C}$ stretching mode at $1,657\text{ cm}^{-1}$ identified above as a measure of *cis*-unsaturation. The identity of the $1,112\text{-cm}^{-1}$ band as a skeletal mode of the acyl chain is further confirmed by its presence in the spectra of ceramide and cerebroside, its absence in sphingosine, and its insensitivity with respect to both intensity and frequency to equilibration of kersin with D_2O .

The spectrum of well annealed, solid *N*-lignoceryl-DL-dihydrogalactocerebroside, a synthetic cerebroside with a saturated C_{24} acyl chain, displays an asymmetric feature at $1,110\text{ cm}^{-1}$ with a shoulder at $1,106\text{ cm}^{-1}$ (spectrum not shown), along with the transitions at $1,060$ and $1,131\text{ cm}^{-1}$. A very weak feature at $1,087\text{ cm}^{-1}$ indicates that the alkyl chains exist in the predominantly all-*trans* conformation. We assign the $1,110\text{-}$ and $1,106\text{-cm}^{-1}$ components to $\text{C}-\text{C}$ stretching modes for the C_{24} and C_{16} chains, respectively. The intensity of the $1,110\text{-cm}^{-1}$ feature is 22% of that of the $1,112\text{-cm}^{-1}$ feature in natural kersin, based on band areas normalized to the $1,130\text{-cm}^{-1}$ peak. This percentage gives a crude estimate of how much of the $1,112\text{-cm}^{-1}$ feature may be attributed to contributions other than the all-*trans* C_{15} and C_9 segments of the nervonic acid residue of kersin. We do note, however, that extremely well-ordered, polycrystalline samples of DL-DPPC, L-DPPC, and dipalmitoyl glycerol exhibit a Raman spectral feature at $1,110\text{ cm}^{-1}$ (I. W. Levin and I. R. Hill, unpublished data). In these compounds, the $1,110\text{ cm}^{-1}$ feature reflects either close-packing effects among C_{16} chains or a $\text{C}-\text{C}$ skeletal stretching motion associated with the glyceryl carbon backbone. A similar contribution to the $1,112\text{-cm}^{-1}$ band in the cerebroside spectra might arise from similar chain packing effects or from the $\text{C}(1)-\text{C}(3)$ segment of the sphingosine moiety. In the present cerebroside systems, we consider the ratio of peak heights at $1,130$ and $1,112\text{ cm}^{-1}$, relative to that at $1,090\text{ cm}^{-1}$, $(h_{1,130} + h_{1,112})/h_{1,090}$, to represent the inclusive measure of all the all-*trans* chain conformers.

According to the plots in Figs. 3 and 4, phrenosin forms the solid and kersin the gel phase with the most nearly extended chains.

A weak band at $1,102\text{ cm}^{-1}$, most clearly visible in solid state phrenosin (Fig. 6), is assigned as a marker of all-*trans*, 18-carbon saturated chain segments (11, 15), which are most numerous in phrenosin (see legend to Fig. 1). Similarly, a weak band at $1,092\text{ cm}^{-1}$, seen in all cerebroside compounds including ceramide and sphingosine (in which it is particularly strong), is assigned as a $\text{C}-\text{C}$ stretching mode of the terminal, all-*trans*, 14-carbon alkyl chain of the sphingosine moiety. Similar modes are seen in distearoyl and dimyristoyl phosphatidylcholine gels at low temperatures (11). Neither of these bands is used as a parameter of all-*trans* chain content.

The five order parameters for chain configuration in the solid phase cerebroside, plotted in Fig. 3, form line patterns similar to one another in shape, but with decreasing degrees of order for phrenosin, kersin, and the natural cerebroside. In contrast, the plotted values of each parameter for the ceramide solid phase yield a different line pattern. The display of the spectral data in this manner indicates that the solid phases of cerebroside appear similar to one another in details of chain packing, but are different from the ceramide. Except for a small crossover for the parameter $\Delta\nu_{3/4}(2,850)$, the line pattern for phrenosin reflects the most highly ordered solid phase.

The line pattern produced on plotting the spectral data for gel phase kerosin (Fig. 4) is similar to that for solid phase kerosin except for a narrowing of the $1,450\text{-cm}^{-1}$ band (methylene CH_2 deformation modes) implying increased order. Except for this parameter, the parameter values lie within 88–99% of those for the solid phase, reflecting a slight loss of order in the gel. Gel phases of phrenosin and natural cerebroside yield line patterns similar to one another (Fig. 4), particularly in exhibiting narrower $2,850\text{-cm}^{-1}$ bands, which indicates an expansion of the chain lattice. The lower values of nearly all other parameters indicate a greater loss of order compared to the solid phase of these compounds (Fig. 3) and to the gel phase of kerosin. For the phrenosin gel, order parameters range from 50 to 83% of those of the solid phase; for the cerebroside gel, parameters range from 66 to 99% of those of the solid phase, with the exception of a higher (122%) value of $1/\Delta\nu_{1/2}(1,450)$.

The line pattern for a gel at 24°C of distearoyl lecithin (DSPC), chosen as a lipid comparable to the cerebroside in having 32 chain methylene carbons per molecule, is also plotted in Fig. 4. The temperature of 24°C was chosen as that for which the values for the order parameters of this gel lie near those of cerebroside. The line pattern for DSPC differs from those of any of the cerebroside gels, showing relatively high values of $h_{2,880}/h_{2,850}$ and $h_{1,062}/h_{1,088}$, indicating a high chain symmetry broken by very few *gauche* rotamers. The low values of $\Delta\nu_{3/4}(2,850)$ and $1/\Delta\nu_{1/2}(1,450)$ indicate that methylene groups on adjacent chains are not interacting with each other in the same geometry as those of any of the cerebroside gels.

Cerebroside is polymorphic in solid and gel states (3, 4). The structures of the solid phases examined here were determined by comparing the phase transition temperatures, determined calorimetrically by us, to those of the phase vs. temperature diagrams determined in x-ray diffraction studies by Abrahamsson and coworkers (3) for synthetic cerebroside containing C_{18} acyl chains. The kerosin and phrenosin fractions studied here gave the complete phase transition patterns of Figs. 8 and 11, respectively, of reference 3. Characteristic transition temperatures were up to 10°C lower than those given for the synthetic cerebroside, a result consistent with chain heterogeneity in the natural compounds. Natural kerosin underwent its first phase transformation at 89°C , compared to 100°C for synthetic kerosin, defining its initial state as isomorphic to state *A* of synthetic kerosin. Natural phrenosin transformed to a new state at 64°C , compared to 73°C for synthetic phrenosin, defining its initial state as isomorphic to state *D* of the latter. The calorimetrically determined phase diagram of natural cerebroside was isomorphic to that of the phrenosin fraction, a result consistent with those of Abrahamsson and coworkers (3).

Phase *A* of synthetic kerosin has a 55-\AA long-spacing (i.e., vertical chains) and exhibits a set of very short short-spacing lines including the shortest ones (3.65 and 3.8 \AA) observed for solid kerosin phases. Phase *D* of phrenosin also exhibits the shortest short-spacings, including a strong 3.7-\AA line, of the solid phrenosins, but in contrast to phase *A* of kerosin, the 43-\AA long-spacing indicates a substantial chain tilt. The chain tilt accommodates the expanded molecular area required by the hydrogen-bonding scheme involving the phrenosin headgroup region, including the 2-OH group of the acyl chain.

The condensed, well ordered nature of solid phase kerosin and phrenosin is a reasonable consequence of the cold-annealing procedure employed here, and is also consistent with these fractions having been purified out of mixed solvents (3).

From the similar magnitudes of the Raman spectral order parameters, including the width of the $2,850\text{-cm}^{-1}$ peak and the unaltered amide I band pattern, we deduce that the gel phase of kerosin is very similar to that of the solid, and contains chains vertical, or only slightly tilted, relative to the bilayer plane. The exceptional parameter, the higher value of $1/(\Delta\nu_{1/2}(1,450))$ in the gel phase of kerosin, indicating a greater constraint of the methylene CH_2 deformation modes relative to the solid, may reflect a slight change in packing and a consequent change in chain tilt. The gel phase of phrenosin shows, according to the Raman spectral order parameters (Fig. 4), in contrast, a relatively greater loss of order compared to the solid; and an expanded chain lattice, as reflected in the large drop in $\Delta\nu_{3/4}(2,850)$. Such a lattice expansion would be required, if, for example, the headgroup area requirement did not alter significantly upon hydration, but the tilt angle decreased from that of the solid phase. X-ray studies are required to establish the nature of the gel phases, including the lamellar repeat distance (long-spacing) and chain tilt.

Single-crystal, x-ray structure determination of a synthetic phrenosin (1) shows that the chains occupy a hybrid lattice, tilted at 49° toward the bilayer surface. Consistent with this structure, the Raman spectra of solid phase, natural phrenosin examined here did not display either of two paraffin lattice parameters, a split $2,850\text{-cm}^{-1}$ mode characteristic of pure triclinic chain packing, or a $1,420\text{ cm}^{-1}$ band characteristic of pure orthorhombic packing.

Kerosin-Dimyristoyl Phosphatidylcholine Mixtures

The Raman spectra of kerosin-DMPC mixtures were examined at two points in the temperature-composition phase diagram: at a mole fraction of kerosin, X_k , of 0.29 at 29°C ; and at X_k equal to 0.7 at 25°C . At the first composition point, the gel to liquid crystalline phase ratio is 1:2, and the value of X_k in gel and liquid crystalline states is 0.65 and 0.10, respectively. Most of the kerosin is in the gel state. At the second composition point, only the gel phase exists and the components are miscible (M. R. Bunow, manuscript in preparation).

The Raman spectra in the $1,700\text{-}$ to $1,600\text{-cm}^{-1}$ region for these samples are shown in Fig. 5. For X_k equal to 0.7, the amide I band is still centered at $1,647\text{ cm}^{-1}$. For X_k equal to 0.29, the amide I band is broadened and shifted to $1,643\text{ cm}^{-1}$. This behavior is consistent with the disruption of the homogeneous amide bond conformation by introduction of DMPC headgroups and by progressively greater *gauche* conformer formation. For comparison, the broad amide I band centered at $1,642\text{ cm}^{-1}$ in ceramide, which lacks a galactose headgroup to "fix" the conformation, is shown in Fig. 5.

The ratio $h_{1,112}/h_{1,060}$, representing the ratio of all-*trans* conformers in the unsaturated acyl chain relative to the total of all-*trans* chain conformers, drops from an apparent value of 0.40 in the kerosin gel to 0.23 in the kerosin-DMPC gel at X_k equal to 0.7 (Fig. 6). The latter ratio can be normalized to 0.31 on the basis of all-*trans* chains contributed only by kerosin to the $1,060\text{-cm}^{-1}$ peak. The accommodation of the C_{14} chains of DMPC in the kerosin bilayer would be expected to result in a lower lateral packing density between $\text{C}(15)$ and $\text{C}(24)$ of the kerosin acyl chains, necessitating expansion of the area occupied by the chains by formation of more *gauche* conformers. The drop in the ratio $h_{1,112}/h_{1,060}$ is consistent with this behavior. The loss in this ratio may be underestimated, because the $1,112\text{-cm}^{-1}$ peak incorporates baseline contributions from the broadened $1,130\text{-cm}^{-1}$ peak (representing other *trans* conformers) and the $1,088\text{-cm}^{-1}$ mode (representing *gauche* conformers). For the kerosin-DMPC mixture at

$X_k = 0.29$, it is difficult to accurately estimate the residual $1,112\text{-cm}^{-1}$ peak magnitude; the peak itself is not resolved (Fig. 6).

Order parameters for the kerosin-DMPC mixtures are given in Fig. 7. As expected, the mixtures shown increasingly reduced order with increasing mole fraction of the shorter-chain phospholipid.

DISCUSSION

The enthalpy of the gel to liquid crystalline phase transition in kerosin is remarkably higher than that for phrenosin and natural cerebroside (~ 16 vs ~ 7 kcal/mol [4]). We assume that the liquid crystalline states of cerebroside and its kerosin and phrenosin fractions are similar just above the phase transition temperatures of $65^\circ\text{--}72^\circ\text{C}$ and that the different phase transition enthalpies primarily reflect profoundly different gel phase structures. The Raman spectral parameters given here (in the results and Fig. 4) for the gel phase of kerosin are consistent with it being the most highly ordered gel phase and hence exhibiting the greatest heat uptake on transforming to a liquid crystalline phase. The primary factor leading to a loss of order in the phrenosin gel appears to be the presence of the spatially perturbing 2-OH group on the acyl chain.

In the Raman spectrum, the amide I band (carbonyl stretching plus in-plane N-H bending motion) occurs at a lower frequency in solid phrenosin than in kerosin ($1,631$ compared to $1,647\text{ cm}^{-1}$), indicating extensive hydrogen bonding. According to the x-ray structure determination of a crystalline synthetic phrenosin, β -D-galactosyl-*N*-(2-D-hydroxyoctadecanoyl)-D-dihydrosphingosine, the amide carbonyl in phrenosin is intermolecularly hydrogen-bonded to one sugar hydroxyl and to the hydroxyl group of a sphingosine moiety (1). The amide nitrogen hydrogen atom is bonded intramolecularly to oxygens of the glycosidic linkage and the fatty acid hydroxyl group. These hydrogen bonds fix a bend in the molecule so that the galactose moiety forms a "shovel" (1). However, in the phrenosin-gel, the Raman spectral amide I band is greatly broadened and shifted upward in frequency, from $1,631 \pm 2\text{ cm}^{-1}$ to $1,640 \pm 5\text{ cm}^{-1}$, indicating loss of the unique hydrogen-bonding scheme seen in the solid phase. This result brings into question the importance of the shovel conformation of the molecules under fully hydrated conditions in the pure phrenosin gel.

In the kerosin fraction, the absence of the 2-OH group on the acyl chain requires that the hydrogen-bonding scheme differ from that described above. The differences are reflected in the higher amide I band frequency, $1,647\text{ cm}^{-1}$. In both solid and gel phases of the natural cerebroside mixture, hydrogen-bonding schemes characteristic of the individual phrenosin and kerosin solid phases appear to survive, as reflected in the presence of amide I bands at both $1,651$ and $1,631\text{ cm}^{-1}$; i.e., hydration has only the effect of slight band broadening in these cases.

The addition of a high proportion of DMPC molecules to kerosin ($X_k = 0.29$) results in a broadening and downward shift of the amide I band. Again, the combination of steric factors imposed by the presence of the DMPC headgroup, and the lattice expansion which occurs in the short-chain phospholipid-kerosin mixture, apparently produces a rearrangement in the hydrogen-bonding scheme.

Some sphingolipids, including some sphingomyelin and cerebroside from brain, contain a

sphingosine and an acyl chain of disparate length (2). The question has been raised whether the longer acyl chains of these sphingolipids are well-enough ordered and extended in natural membranes or hydrated lamellar phases to interdigitate across the central plane of the bilayer and mechanically couple the inner and outer monolayers of the membrane (17). The Raman spectral order parameters (Figs. 4 and 5) supply information for a computation of chain overlap, as follows.

The number of *gauche* conformers in the cerebroside gels can be crudely estimated by comparing the peak height ratio $h_{1,060}/h_{1,088}$ in cerebroside and DSPC gels. For DSPC gels, it has been computed that five to six *gauche* conformers per molecule appear between 10° and 50°C (11). A plot of either $h_{1,088}/h_{1,295}$, where the fairly invariant 1,295-cm⁻¹, methylene CH₂ twisting mode is used as the reference peak, or of $h_{1,088}/h_{1,060}$ against temperature, shows that the number of *gauche* conformers increases in an approximately linear manner with temperature in this temperature range in DSPC gels (plots not shown). Thus, at 25°C, DSPC gels contain about two *gauche* conformers per molecule; and kersin gels, having a higher *trans/gauche* conformer ratio (see Fig. 4), less than two. Noting that for the phrenosin gel at 24°C, the value of $h_{1,060}/h_{1,088}$ of 4.7 is equivalent to that measured for the DSPC gel at 35°C, we estimate there are about four *gauche* conformers per mole in the phrenosin gel. The acyl chain shortens by 1.27 Å per pair of *gauche* conformers (18), while the eight carbons of the C₂₄ acyl chain extend ~8.4 Å beyond the end of the sphingosine moiety. For the cerebroside and kersin and phrenosin fractions, the x-ray data for solid and hydrated phases is consistent with a molecular bilayer model with a polar headgroup surface and an interior, hydrophobic region containing parallel sphingosine and acyl chains (references 1, and 3 and Fig. 21 of reference 8). In particular, natural anhydrous cerebroside, containing C24 acyl chains, gives long-spacings increased by 6 Å, but similar short spacings relative to synthetic phrenosin containing C18 acyl chains (3), consistent with a content of extended, C24 acyl chains overlapping one another beyond carbon 18. Then, with the assumption that all the *gauche* bonds occur in the acyl chain, there would be ~7.1 and 5.8 Å of residual chain overlap in the kersin and phrenosin gels, respectively, at 22°C.

In the kersin-DMPC gel (at X_k of 0.7), it is clear from the reduction in $h_{1,112}/h_{1,060}$ that the coupling by chain overlap is reduced. However, the evidence is inadequate for drawing conclusions about the overlap of sphingolipid acyl chains in natural membranes.

We have assigned the 1,112-cm⁻¹ Raman spectra mode of cerebroside as a parameter of all-*trans* conformers of the long, nervonic acid residues. A similar feature at ~1,111 cm⁻¹ is visible in Raman spectra of fully hydrated bovine brain sphingomyelin up to the gel to liquid crystalline transition temperature (Fig. 2 of reference 19). In the sphingomyelin examined in the latter work (19), 33% of the acyl chains had a C24:1 composition, comparable to the 40%-C24:1 content in kersin. It should be noted that in reference 19 the position of the double bond is, however, incorrectly described. The spectral analogy in cerebroside and sphingomyelin and the correspondence with chain composition lend support to our assignment of the 1,112-cm⁻¹ mode.

In conclusion, the Raman spectral studies of cerebroside reported here provide new information on the conformation of both the chain and headgroup portions of these molecules in hydrated lamellar phases, as referred to the crystalline structures. The results elaborate the effects on packing of chains of the 2-OH group of the acyl chain of phrenosin, and also supply

an estimate of the degree of overlap of the long acyl chains across the central plane of the bilayer.

We thank Dr. N. L. Gershfeld for use of the DSC-2 scanning calorimeter.

Received for publication 3 March 1980 and in revised form 11 August 1980.

REFERENCES

1. PASCHER, I., and S. SUNDELL. 1977. Molecular arrangements in sphingolipids. The crystal structure of cerebroside. *Chem. Phys. Lipids*. **20**:175-191.
2. NORTON, W. T. 1977. Isolation and characterization of myelin. In *Myelin*. P. Morell, editor. Plenum Press, New York. 161-199.
3. ABRAHAMSSON, S., I. PASCHER, K. LARSSON, and K.-A. KARLSSON. 1972. Molecular arrangements in glycolipids. *Chem. Phys. Lipids*. **8**:152-179.
4. BUNOW, M. R. 1979. Two gel states of cerebroside: calorimetric and Raman spectroscopic evidence. *Biochim. Biophys. Acta*. **574**:542-546.
5. O'BRIEN, J. S., and G. ROUSER. 1964. The fatty acid composition of brain sphingolipids: sphingomyelin, ceramide, cerebroside and cerebroside sulfate. *J. Lipid Res.* **5**:339-342.
6. ACHER, A. J., and J. N. KANFER. 1972. A method for fractionating of cerebroside into classes with different fatty acid compositions. *J. Lipid Res.* **13**:139-142.
7. DeVRIES, G. H., and W. T. NORTON. 1974. The fatty acid composition of sphingolipids from bovine CNS axons and myelin. *J. Neurochem.* **22**:251-257.
8. ABRAHAMSSON, S., B. DAHLÉN, H. LÖFGREN, I. PASCHER, and S. SUNDELL. 1977. Molecular arrangement and conformation of lipids of relevance to membrane structure. In *Structure of Biological Membranes*. S. Abrahamsson and I. Pascher, editors. Plenum Press, New York. 1-23.
9. BUNOW, M. R., and I. W. LEVIN. 1977. Comment on the carbon-hydrogen stretching region of vibrational Raman spectra of phospholipids. *Biochim. Biophys. Acta*. **487**:388-394.
10. GABER, B. P., and W. L. PETICOLAS. 1977. On the quantitative interpretation of biomembrane structure by Raman spectroscopy. *Biochim. Biophys. Acta*. **465**:260-274.
11. YELLIN, N., and I. W. LEVIN. 1977. Hydrocarbon chain trans-gauche isomerization in phospholipid bilayer gel assemblies. *Biochemistry*. **16**:642-647.
12. YELLIN, N., and I. W. LEVIN. 1977. Hydrocarbon chain disorder in lipid bilayers. Temperature-dependent Raman spectra of 1,2-diacyl phosphatidylcholine-water gels. *Biochim. Biophys. Acta*. **489**:177-190.
13. SNYDER, R. G., S. L. HSU, and S. KRIMM. 1978. Vibrational spectra in the C-H stretching region and the structure of the polymethylene chain. *Spectrochim. Acta*. **34A**:395-406.
14. HILL, I. R., and I. W. LEVIN. 1979. Vibrational assignments and carbon-hydrogen stretching mode assignments for a series of n-alkyl carboxylic acids. *J. Chem. Phys.* **70**:842-851.
15. LIPPERT, J. L., and W. L. PETICOLAS. 1972. Raman-active vibrations in long-chain fatty acids and phospholipid sonicates. *Biochim. Biophys. Acta*. **282**:8-17.
16. KISHIMOTO, Y., and N. S. RADIN. 1964. Structures of the ester-linked mono- and disaturated fatty acids of pig brain. *J. Lipid Res.* **5**:98-102.
17. SCHMIDT, C. F., Y. BARENHOLZ, C. HUANG, and T. E. THOMPSON. 1978. Monolayer coupling in sphingomyelin bilayer systems. *Nature (Lond.)*. **271**:775-777.
18. TRAUBLE, H. 1972. Phase transitions in lipids. In *Biomembranes*. F. Kreuzer and J. F. G. Slegers, editors. Plenum Press, New York. 3:197-227.
19. FAIMAN, R. 1979. An analysis of band profiles in the Raman spectra of an aqueous dispersion of sphingomyelin. *Chem. Phys. Lipids*. **23**:77-84.